

MARSQUAKE ACTIVITY DRIVEN BY THE SUN? M. Knapmeyer¹, S. C. Stähler², I. Daubar³, F. Forget⁴, A. Spiga⁴, T. Pierron⁴, M. van Driel², D. Banfield⁵, E. Hauber¹, M. Grott¹, N. Müller¹, C. Perrin⁶, A. Jacob⁶, A. Lucas⁶, B. Knapmeyer-Endrun⁷, C. Newman⁸, M. P. Panning⁹, R. C. Weber¹⁰, F. J. Calef⁹, M. Böse², S. Ceylan², C. Charalambous¹¹, J. Clinton², D. Giardini², A. Horleston¹², T. Kawamura⁶, A. Khan², M. Lemmon¹⁴, R. Lorenz¹⁵, W. T. Pike¹¹, J.-R. Scholz¹³, P. Lognonné⁶, B. Banerdt⁹;

¹DLR, Rutherfordstr. 2, 12489 Berlin, Germany, martin.knapmeyer@dlr.de, ²Institute of Geophysics, ETH Zürich, Sonneggstrasse 5, 8092 Zürich, Switzerland, ³Department of Earth, Environmental, and Planetary Sciences, Brown University, Campus Box 1846, Providence, RI 02912-1846, USA, ⁴Laboratoire de Météorologie Dynamique / Institut Pierre Simon Laplace (LMD/IPSL), Sorbonne Université, Centre National de la Recherche Scientifique (CNRS), École Polytechnique, École Normale Supérieure, ⁵Cornell University, Cornell Center for Astrophysics and Planetary Science, Ithaca, NY, 14853, USA, ⁶Université de Paris, Institut de physique du globe de Paris, CNRS, F-75005 Paris, France, ⁷Bensberg Observatory, University of Cologne, Vinzenz-Pallotti-Str. 26, 51429 Bergisch Gladbach, Germany, ⁸Aeolis Research, 333 N Dobson Road, Unit 5, Chandler AZ 85224-4412, USA, ⁹Jet Propulsion Laboratory, California Institute of Technology; 4800 Oak Grove Dr., M/S 183-301, Pasadena, CA 91109, USA, ¹⁰NASA MSFC, NSSTC Mail Code ST13, 320 Sparkman Drive, Huntsville, AL 35805, USA, ¹¹Department of Electrical and Electronic Engineering, Imperial College London, South Kensington Campus, London, SW7 2AZ, United Kingdom, ¹²School of Earth Sciences, University of Bristol, Wills Memorial Building, Queens Road, Bristol BS8 1RJ, UK, ¹³Max Planck Institute for Solar System Research, Justus-von-Liebig-Weg 3, 37077 Göttingen, Germany, ¹⁴Space Science Institute, 4765 Walnut Street, Suite B, Boulder, CO 80301, USA ¹⁵Johns Hopkins Applied Physics Laboratory, 11100 Johns Hopkins Road, Laurel, MD 20723, USA

Introduction: Studies on Martian endogenous seismic activity prior to the InSight mission were mainly concerned with the size-frequency distribution of expected marsquakes and the resulting seismic moment release rate. Occurrence times were rarely discussed, but probably assumed to be as unpredictable as those of major earthquakes. This is certainly true for [1], but most likely also for most other studies (e.g. [2][3][4], to name but a few). An exception is [5], where seismicity induced by solar and phobosian tides is predicted.

The family of High Frequency seismic events (HF, classification scheme of [6]) recorded by the InSight SEIS experiment [7] shows a detection rate that is highly variable with time, and somewhat anti-correlated to the seasonal variability of wind induced background noise.

We show that the wind noise variation does not explain the variability of event detections, and that a true variability of seismic activity exists on Mars.

Data: Between 12. Jan. 2019 and 31. Aug. 2020, InSight detected 415 HF events. A careful selection is necessary to avoid observational biases. We discard all events with indiscernible arrivals, or which might be of non-seismic origin (quality "D", [6]). According to the distribution of recorded amplitudes and signal-to-noise ratios (SNR), and to inferred catalog completeness thresholds, we discard all events with amplitudes more than 215 dB below a reference displacement of 1 m, or with SNR below 2.56. We also discard all events recorded prior to 01. June 2019, when the sampling rate of continuously downlinked data was increased from 10 Hz to 20 Hz. The majority of HF events would be visible in the 10 Hz data stream as well, but since the event rate started rising at about this time, we rule out an observational bias by not using the 10 Hz data here. What remains are 118 events that were recorded between 01. June 2019 and 31. Aug. 2020. Figure 1a shows their cumulative count (square symbols).

Methods: Lacking information about source location and mechanism, it is currently not possible to constrain the stress regimes under which events occur. We can only conduct maximum likelihood analyses of plausible driving processes that exhibit a variability in time similar to the changing event rate. Akaike Information Criterion and evidence ratio (probability that a model is not recognized as the best one due to stochastic properties of the available data [8]) are used to rank processes and assess the ranking's credibility.

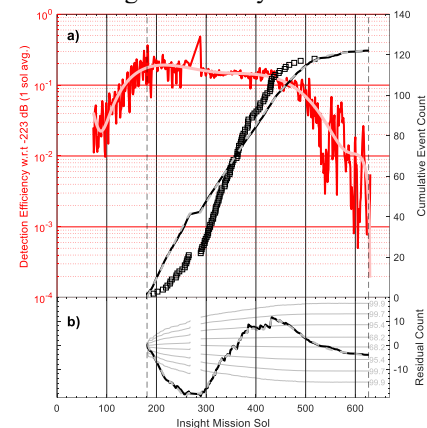


Figure 1 Detection efficiency (fraction of detected events) and residual event count. (a) Red: sol-by-sol detection efficiency, pink: 7th degree polynomial fit. Squares: cumulative HF event count, with gap during the 2019 solar conjunction. Black line: cumulative count assuming a constant event rate that yields the number of observed events, using the red efficiency curve. Dashed grey: as black, but using the polynomial efficiency model. (b) Black: residual between observed cumulative count in and black curve of (a). Dashed grey: residual between observed count and dashed grey curve in (a). Light grey: percentile contours corresponding to 1 ... 5 σ of a Gaussian distribution, showing sampling uncertainty range.

Proof of variable event rate: From the distribution of amplitudes we estimate how the number of detections depends on noise level, and simulate cumulative event counts resulting from a constant event rate (Figure 1a). We find that there is a considerable and variable residual detection count, which is extremely unlikely (beyond 99.9% level) to be observed when the occurrence rate is constant (Figure 1b).

This procedure also gives rise to a detection efficiency factor $0 \leq \eta \leq 1$ by which a model event rate has to be multiplied before comparison with the observed event sequence: a fraction η of the actually occurring events is detected by InSight. A 7th degree polynomial captures sufficient detail of the sol-by-sol noise average to compute a useful η (Figure 1a).

Impacts: It has been suggested (e.g. [9]) that an increase of the meteorite impact rate might occur if Mars is near aphelion. However, we do not yet have an unambiguous observation of seismic impact signals that would allow judging if HF events are impacts. We lay aside this question for now.

Phobos Tides: A spike train Fourier transform of event occurrence times, as used to determine periodicities in Deep Moonquake activity [11], does not exhibit peaks at periods connected to the orbit of Phobos (contrary to the prediction of [5]). We rule out Phobos tides as driver of HF events.

Solar Tide: Annual solar tides were discussed by [2] and [5], who arrive at opposite conclusions. We thus analyze a rate model based on the annual solar tide. (A possible effect of daily solar tides is not accessible due to the strong daytime winds, which cover all other diurnal variations by preventing any event detection.)

CO₂ ice load: The polar ice caps of Mars are well known to show a strong seasonal variation of their extent, which is due to evaporation and deposition of CO₂ ice, as reflected by atmospheric pressure [12]. Taking this as analogy to reservoir induced seismicity on Earth, we analyze a rate model driven by the annual atmospheric pressure cycle as proxy for the ice load cycle.

Illumination: Change of illumination, and thus solar heat influx on steep topography, may lead to thermal erosion and mass wasting. Although landslides are inefficient seismic sources, we analyze a rate model driven by the areocentric longitude of the Sun as marker for Martian seasons.

Conclusions: A constant event rate cannot explain the sequence of observed HF events. There is also no indication for a connection to Phobos' tides. The observations cover only about 2/3 of a Martian year and do not allow for a conclusive decision, but evidence is in favor for a seasonal driving force that is connected to solar illumination. This suggests extreme illumination/shadowing conditions in the HF source region(s). Changes of CO₂ ice load, and annual solar tides are less likely explanations of the observed variability (i.e. have

higher evidence ratios, Figure 2), but cannot be ruled out yet. Observation of additional activity cycles will likely help discriminating models.

The unexpected seasonality of marsquakes indicates that there is new science of ongoing geological processes on Mars, waiting for further investigation.

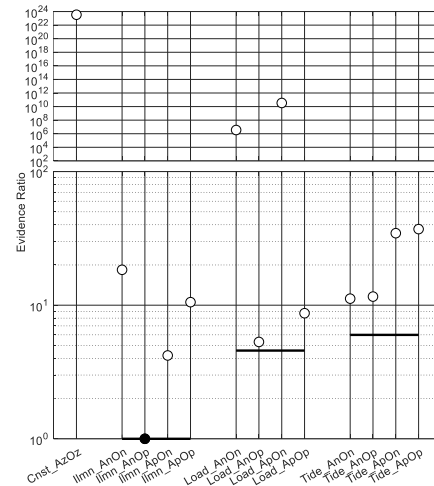


Figure 2 Evidence ratios for the analyzed models (circles) and model groups (bars). Model names consist of 4 letters for model type (Cnst - constant rate, Ilmn - Illumination, Load - Ice load, Tide - annual solar tide) and a code for a parameter space quadrant (Amplitude factor (A) vs. DC offset (O), positive (p) or negative (n)). The best model is Ilmn_AnOp (filled circle). The evidence ratio tells how much less likely a model is mistakenly not identified as the best one due to sampling uncertainty.

Acknowledgements: We acknowledge NASA, CNES, partner agencies and Institutions (UKSA, SSO, DLR, JPL, IPGP-CNRS, ETHZ, IC, MPS-MPG) and the operators of JPL, SISMOC, MSDS, IRIS-DMC and PDS for providing SEED SEIS data. The event catalog used in this study is based on the data recorded by the SEIS instrument on Mars [7]. Noise RMS amplitudes and event catalog [6] are based on waveform data which is released to the public via the NASA Planetary Data System (pds.nasa.gov/) and IRIS several times a year (www.iris.edu/hq/sis/insight).

References: [1] Knapmeyer et al. (2006) JGR, 111, E11006. [2] Philips (1991) LPI/TR-91-02. [3] Golombek et al. (1992), Science, 258, 979-981. [4] Plesa et al. (2018) GRL, 45, 2017GL076124. [5] Manga et al. (2019) GRL, 46, 6333-6340. [6] Clinton et al. (2020), PEPI, in press [7] Lognonné et al. (2019), SSR, 215, 12 [8] Burnham et al. (2011) Behav. Ecol. Sociobiol. 65, 23-35. [9] Ivanov (2001) SSR, 96, 87-104. [10] Daubar et al. (2020) JGR, 125, 8. [11] Bulow et al. (2007), JGR, 112, E09003. [12] Hess et al. (1979), JGR, 84, 2923-2927.